

# Reorientational Dynamics and Intermolecular Cooperativity of Reactive Polymers. 1. Model Epoxy–Amine Systems

Benjamin Fitz, Saša Andjelić, and Jovan Mijović\*

Department of Chemical Engineering, Chemistry, and Materials Science,  
Polytechnic University, Six Metrotech Center, Brooklyn, New York 11201

Received January 7, 1997; Revised Manuscript Received May 3, 1997

**ABSTRACT:** An investigation was conducted to determine how the advancement of chemical reactions and the prepolymer molecular weight affect the reorientational dynamics and intermolecular cooperativity in model epoxy–amine systems. Experimental results were obtained by dielectric spectroscopy over a wide range of frequency and temperature. A strong effect of the progress of reaction on reorientational dynamics was noted and an explanation was put forward within the framework of the coupling theory, marking the first time this concept was applied to reactive systems. It was proposed that the molecular-level characteristics that govern the intermolecular cooperativity of reactive systems can be classified into two categories: (1) molecular architecture, determined by molecular symmetry, rigidity, and steric hindrance, and (2) dielectric architecture, determined by the type and concentration of all dielectrically active species. Both molecular and dielectric architecture vary in the course of chemical reaction, and the overall direction in which the cooperativity shifts is governed by the interplay between these two phenomena.

## Introduction

Reorientational dynamics of glass-forming polymers and small molecules are currently the subject of extensive experimental and theoretical studies in a number of laboratories worldwide.<sup>1–11</sup> However, information on the reorientational dynamics in systems that undergo a temporal evolution of structure as a result of chemical reactions is scarce.<sup>12–17</sup> A systematic investigation of the dynamics of reactive systems, polymer-forming and non-polymer-forming alike, is currently underway in our laboratory.

The advancement of chemical reactions alters the very nature of the material and adds a new component to the study of dynamics of molecular motions in polymers. Changes in the chemical composition, glass transition temperature ( $T_g$ ), cross-link density, and morphology are accompanied by a continuous variation in the time scale of the segmental motions. Consequently, the origin and the characteristic relaxation times of various molecular processes, their temperature dependencies, activation energies, and the widths and breadths of their distributions all change with the progress of reaction. A fundamental understanding of the relaxation dynamics in reactive systems and their relation to the chemophysical characteristics of the evolving structure poses an exciting experimental and theoretical challenge and has provided incentive for this research.

The various dielectric relaxations are not always consistently defined in the literature, and hence a brief description of their molecular origin is included here. The major dielectric relaxation in polymers with permanent dipoles is termed  $\alpha$  relaxation—its molecular origin lies in the segmental motions. Since the principal role in determining the glass transition is played by the time scale of the segmental motions, and not the Rouse and/or sub-Rouse modes,  $\alpha$  relaxation is associated with the “dielectric glass transition”. Secondary relaxations, labeled  $\beta$ ,  $\gamma$ , etc., in the order of decreasing temperature (at constant frequency) or increasing frequency (at constant temperature) are associated with localized

motions in the glassy state. It is also important to point out that  $\alpha$  and  $\beta$  relaxations have different molecular origins but are interrelated, since the same dipoles contribute to both processes. In some polymers, under certain conditions, it is possible to distinguish between different types of dipoles (or components of the same dipole) on the basis of their location and orientation in the electric field. Stockmayer<sup>18</sup> has classified all dipoles into three categories type A, oriented parallel to the chain contour; type B, oriented perpendicular to the main chain; and type C, located in the side chain. A well-known and widely studied example is *cis*-polyisoprene, which contains type A and B dipoles whose relaxations can be resolved in the frequency domain.<sup>19–21</sup> The important point here is that the relaxation of type B dipoles in polymers is associated with segmental motions and is therefore synonymous with  $\alpha$  relaxation. Type A dipoles give rise to a relaxation at lower frequency (at constant temperature) with the characteristic relaxation time that is affected by the fluctuations of the end-to-end vector and is therefore of the molecular weight. This relaxation is often referred to as normal mode. Another relaxation at a temperature higher (at constant frequency) than that of the  $\alpha$  relaxation was reported in crystalline polymers and is assigned to the molecular motions of amorphous entities within the crystalline phase.<sup>22</sup> Neither this relaxation nor the thermal mode is identified in a consistent manner by a Greek letter in the literature.

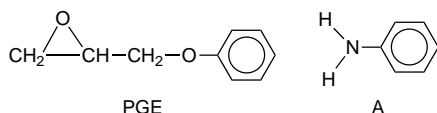
The principal goal of the first of two parts of this communication is to examine how the advancement of chemical reactions in an epoxy–amine model system and the increase in molecular weight in a homologous series of epoxy prepolymers affect the reorientational dynamics within the general framework of intermolecular cooperativity. In the paper that immediately follows we describe our results for a series of network-forming multifunctional epoxy–amine formulations.

## Experimental Section

**Materials.** The non-polymer-forming model epoxy–amine system consisted of 1,2-epoxy-3-phenoxypropane, also known as phenyl glycidyl ether (or PGE), and aniline. Their chemical structures are shown in Table 1. Both compounds were

\* To whom correspondence should be addressed.

© Abstract published in *Advance ACS Abstracts*, August 1, 1997.

**Table 1. Chemical Structure of 1,2-Epoxy-3-phenoxypropane (PGE) and Aniline**

supplied by Aldrich. All PGE–aniline mixtures contained the stoichiometric amount of epoxy group and amine hydrogen, corresponding to the PGE:aniline molar ratio of 2:1. The components were mixed at room temperature, heated until a clear mixture was obtained, and immediately tested under a series of conditions of different frequencies, temperatures, and times. For temperature scans the samples were quenched from above the  $T_g$  to the low initial temperature and heated at a constant rate of 2 °C/min. For frequency sweeps, the samples were quenched to the lowest measurement temperature, allowed to thermally equilibrate, and then swept. All subsequent higher measurement temperatures were arrived at by heating at 2 °C/min.

The six epoxy prepolymers utilized in this study were all based on diglycidyl ether of Bisphenol A (DGEBA). Their commercial names, chemical structure, degree of polymerization ( $\bar{x}$ ), and molecular weight (MW) are listed in Table 2. For testing, these materials were heated to the liquid state, introduced into the measurement cell, and quenched to a desired temperature. Note that all these prepolymers can be readily supercooled.

**Techniques.** Our experimental facility for dielectric measurements consists of modified commercial and custom-made (in-house) instruments. The three commercial instruments are (1) a Solartron 1260 impedance/gain phase analyzer (10  $\mu$ Hz to 32 MHz), (2) a Hewlett-Packard 4284A precision LCR meter (20 Hz to 1 MHz), and (3) a Hewlett-Packard 8752C network analyzer (300 kHz to 1.3 GHz). Each instrument was modified by the addition of a temperature-controlled chamber and interfaced to a computer via a National Instruments IEEE 488.2 interface bus. Two- and three-electrode cell configurations were utilized for the measurements below 10 MHz and are described elsewhere.<sup>23,24</sup> Measurements performed in the network analyzer made use of specially designed coaxial probe and our own software to calculate dielectric constant and loss from the measured reflection coefficient. A limited number of runs was performed between 15 and 85 GHz on a state-of-the-art equipment assembled at Polytechnic and described elsewhere.<sup>25</sup> The Solartron impedance/gain phase analyzer was further modified by the addition of a high-impedance adapter (HIA), assembled in our laboratory, which becomes necessary when the measured impedance exceeds the upper limit of the analyzer (100 M $\Omega$ ). Studies of cross-linking, for instance, cannot be carried out beyond that point without the HIA. High-impedance samples unduly load the instrument, the output voltage drops below the expected value, and spurious measurements are reported. To circumvent that, the HIA provides, by the way of two unity-gain buffers, impedance of 20 G $\Omega$  with respect to the sample and 2  $\Omega$  with respect to the analyzer. Schematics of the entire setup (for low- and high-frequency tests) and the HIA are given in Figure 1, with further details available elsewhere.<sup>26</sup> Most of our data are presented in the frequency domain in terms of the complex dielectric permittivity,  $\epsilon^*(\omega)$ , or the complex dielectric susceptibility,  $\chi^*(\omega)$ , which is defined by  $\epsilon^*(\omega) = 1 + 4\pi\chi^*(\omega)$ . Some supporting evidence was obtained from differential scanning calorimetry (DSC) and Fourier transform infrared (FTIR) spectroscopy. DSC was performed with TA Instrument Co. model 2920 at a heating rate of 10 °C/min, and FTIR spectroscopy was conducted as described previously.<sup>27</sup> A Waters model 590 was used for size exclusion chromatography measurements (at 1 mL/min in THF).

## Theoretical Background

The interpretation of the dielectric response of materials in the majority of published studies has, as its

starting point, the classic Debye response, despite the fact that such response is seldom encountered in simple liquids, hardly ever in polymers (for an exception see ref 28), and never in solids. The experimentally observed results are treated as departures from the Debye behavior and are most commonly “explained” in terms of distributions that are quantified by adjusting some of the many parameters at one’s disposal so as to make the model “fit” the data. Various empirical expressions with one or more adjustable parameters (e.g., Cole–Cole, Cole–Davidson, Havriliak–Negami) have been used to fit the data with great accuracy, but the physical plausibility of the concept of the distribution of relaxation times remains clouded by the inability of those equations to provide an insight into the molecular nature of the relaxation processes. Furthermore, a mathematically evaluated distribution function, by its nature, does not contain more information than the experimental function from which it was obtained.

The fundamental argument should begin with the proposition that the relaxation processes are governed by cooperativity, with the ideal Debye response representing the limiting case of a noncooperative or non-interacting system. Cooperative interactions are the fundamentally dominant and not the modifying influence on the dielectric behavior, and hence the correct route is to start with the essential characteristic of all relaxation phenomena, i.e., the interactive nature of the relaxation process (e.g., refs 29–34). Small deviation from the ideal Debye response could be modeled by means of correlation functions or by superposition of Debye responses, though even in such instances the superposition of single relaxation processes remains fundamentally different from the relaxation process governed by the cooperative interactions.

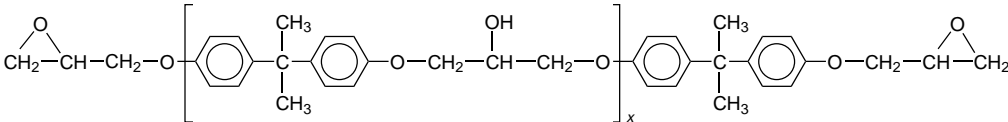
In general, cooperativity dictates that a number of molecular segments or moieties respond in unison to an applied signal (electric field in this study) in order for a relaxation to take place. The extent to which cooperativity is required depends on many factors that include both molecular characteristics (e.g., chemical composition, type, and concentration of dielectrically active moieties, specific interactions, molecular architecture, microstructure) and external variables (e.g., temperature, pressure). The intermolecular cooperativity obviously changes with the progress of reactions, and our goal is to establish how that can be best understood. In this study we shall seek to interpret the changes in the cooperativity in reactive systems by invoking primarily Ngai’s coupling theory<sup>30</sup> and, on several occasions, Jonscher’s many-body interaction theory.<sup>31</sup> The salient features of these formalisms are recapped below.

Jonscher’s argument is centered around the experimentally observed universality of the dielectric behavior, which is rooted in the interactive many-body dynamics. The concept of many-body interactions, as interpreted by Jonscher, has led to the development of a rigorous theory by Dissado and Hill.<sup>35</sup> The principal tenet of Jonscher is that the frequency dependence of the dielectric loss peak is not exponential; instead, it could be universally represented by two power laws combined into the following equation:

$$\chi''(\omega) \propto 1/[(\omega/\omega_p)^{-m} + (\omega/\omega_p)^{1-n}] \quad (1)$$

where  $\chi''$  is the imaginary susceptibility,  $\omega_p$  is the peak frequency, and  $m$  and  $n$  are the power law exponents that fall in the range between 0 and 1. Jonscher views

**Table 2. Chemical Structure, Source, Molecular Weight (MW), Degree of Polymerization ( $x$ ), and the Power Law Parameters  $m$  and  $n$** 

				
trade name	$M_w$ (g/mol)	$x$	$n$	$1 - m$
Epon 825	360	0.1	0.87	0.50
Ciba-Geigy GY 6010	375	0.15	0.77	0.48
Ciba-Geigy GY 6020	400	0.25	0.75	0.45
Ciba-Geigy GT 7071	980	1.0	0.49	0.37
Ciba-Geigy GT 7013	1380	2.3	0.46	0.34
Ciba-Geigy GT 7074	2100	4.0	0.44	0.33
Ciba-Geigy GT 7097	6100	9.0	0.415 <sup>a</sup>	0.37

<sup>a</sup> This is the average value between two slopes

the observed frequency dependence as a universal consequence of the many-body interactions and, consequently, makes no reference to any distribution of parameters. The exponents  $m$  and  $n$  (eq 1) represent two separate and independent processes. The Dissado–Hill theory relates these exponents to the degree of correlations between flip and flip-flop transitions, respectively, both of which result from the short range dynamics. It is important to emphasize, however, that the two slopes have physical significance in relation to cooperativity. The flattening of the loss peak is a measure of the increase in rigidity and a decrease in the extent of uncorrelated interactions. The lack of precisely defined  $m$  and  $n$  as a function of temperature suggests the presence of overlapping mechanisms.

Ngai's concept also starts with the premise that the dynamics in the condensed phase are restricted by intermolecular cooperativity. According to his coupling theory, the segmental relaxation gives rise to a correlation function of the Kohlrausch–Williams–Watts (KWW) type with the temperature dependent relaxation time given as

$$\tau^* = [(1 - n)\omega_c^n \tau_0]^{1/(1-n)} \quad (2)$$

where  $\tau_0$  is the intermolecular uncorrelated relaxation time,  $\omega_c$  is the crossover frequency, and the coupling parameter  $n$  ( $0 < n < 1$ ) is proportional to the capacity of intermolecular coupling, which in turn, depends on the chemical composition. The coupling parameter increases with increasing resistance to the local segmental motions and we shall revert to this later in the text. Ngai and co-workers have also reported on the variation of intermolecular cooperativity with chemical structure but did not look into a reactive system whose structure evolves with time.

## Results and Discussion

**1. Effect of Progress of Reaction in the Model System on Reorientational Dynamics.** We begin the discussion of our results by considering first the dynamics of the individual components and their mixture prior to the onset of chemical reactions. This is an important consideration since mixing could change the nature of the intermolecular cooperativity and hence the time scale of the segmental motions.<sup>36</sup> We first identify the various types of relaxations associated with different moieties in each component (amine and epoxy) separately and then examine the effect of mixing on the relaxations in their mixture before the initiation of reactions.

A differential scanning calorimetry (DSC) thermogram of aniline (model amine) reveals a glass transition at  $-122$  °C and a melting point at  $-6$  °C. Dielectric constant and loss of liquid aniline at  $25$  °C over 14 decades of frequency are shown in Figure 2. This figure shows clearly how the various polarization mechanisms that characterize the dielectric response in the frequency domain can be distinguished according to their frequency dependence. The 14 decades in Figure 2 are conveniently subdivided into four zones labeled A–D. A pronounced increase in dielectric constant below  $10$  Hz reflects the presence of an electrode blocking layer. Between approximately  $10$  Hz and  $0.1$  MHz lies zone B, which is dominated by the polarization due to migrating charges. The translational motions of migrating charges (e.g., ions) is purely dissipative; it contributes to dielectric loss but not permittivity, as clearly seen in the figure. Dielectric loss is inversely proportional to frequency, and the slope of  $-1$  indicates that an R–C parallel circuit, its simplicity notwithstanding, could describe the corresponding dielectric response. Zone C is located between about  $0.1$  and  $10$  MHz and is characterized by a constant permittivity and a negligible loss. Those frequencies are apparently too fast for the translational motions of the migrating charges but still too slow to affect the reorientational dynamics of dipoles, as we observe no dipole loss. At still higher frequencies, however, we enter zone D where the classic dipole relaxation is observed. A Debye function was drawn through data points for clarity. The loss maximum appears at  $9$  GHz, corresponding to a relaxation time of  $17.7$  ps. In sum, Figure 2 is a clear example of the need for data over a wide frequency range for the complete description of polarization due to charge migration and dipole orientation in simple molecules. Dielectric loss of aniline as a function of temperature did not reveal a relaxation peak corresponding to that observed at about  $10$  GHz in the frequency domain at  $25$  °C. This is because aniline is crystalline at a low temperature where that peak would appear.

A DSC thermogram of the supercooled PGE (model epoxy) revealed a  $T_g$  at  $-75$  °C, a two-step crystallization process at  $-40$  and  $-28$  °C, and a melting point at  $3$  °C. Dielectric constant and loss of PGE as a function of temperature, with frequency as a parameter, are shown in Figure 3. As expected, the rapidly rising portion of  $\alpha$  relaxation shifts to higher temperature with increasing frequency. The low-temperature end of the  $\alpha$  relaxation peak marks the onset of the “dielectric  $T_g$ ”; the peak has a sharp maximum because it does not

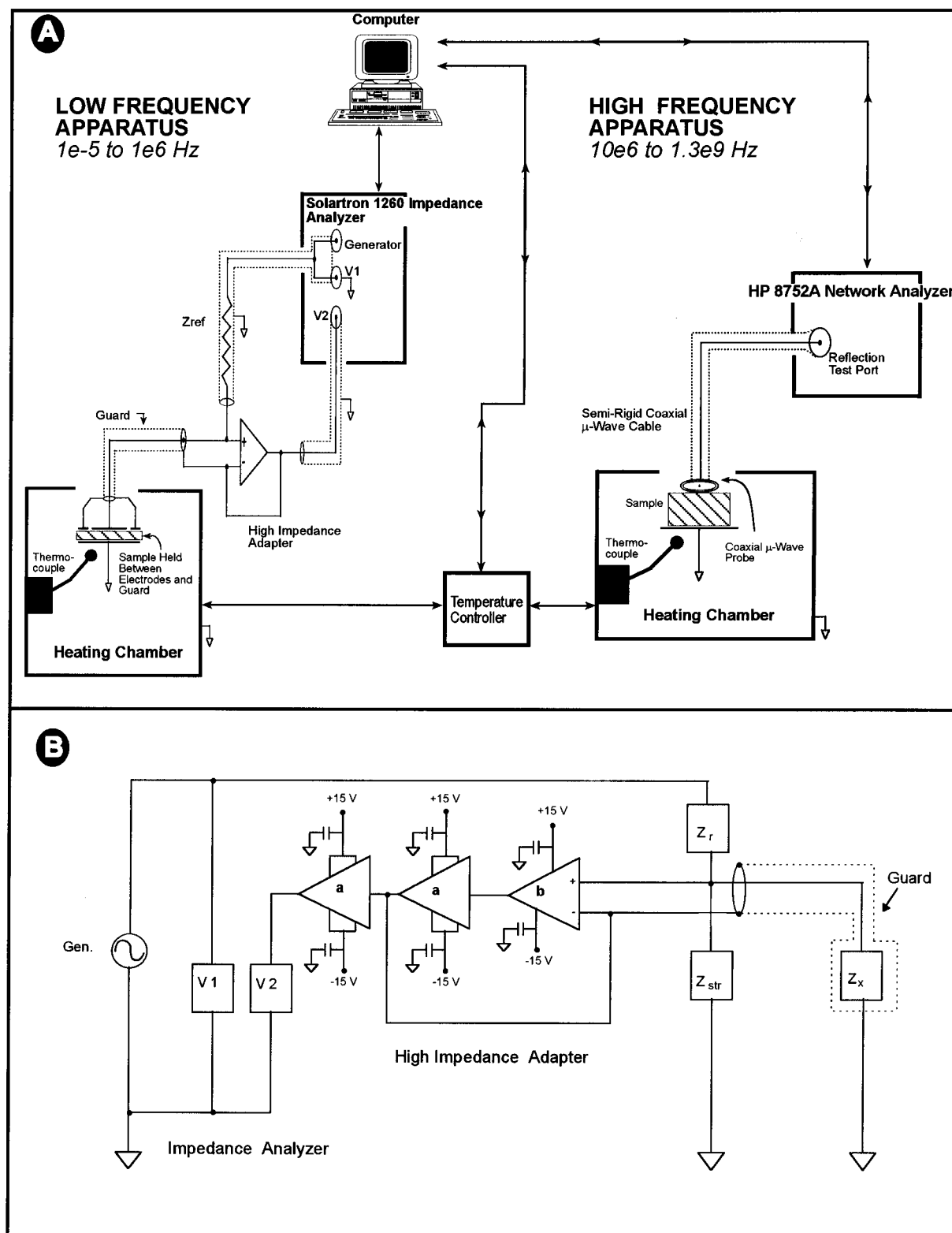


**Figure 1.** (A) Schematic of setup for measurements of dielectric response below 1.3 GHz. (B) Schematic diagram of high-impedance adapter (HIA).

evolve completely due to the onset of crystallization, which interferes with the relaxation process and causes an abrupt drop in the constant and loss. The subsequent increase in dielectric constant and loss that sets in around 0 °C is caused by melting. The loss maximum of liquid PGE at 25 °C is located at 2.5 GHz, corresponding to a relaxation time of 63.7 ps.

Next, a stoichiometric mixture of PGE and aniline was prepared and investigated *before* the onset of

chemical reactions. Dielectric loss as a function of temperature at various frequencies revealed a strong  $\alpha$  relaxation of intensity similar to that in the pure PGE but shifted to a slightly lower temperature (for a given frequency). As expected, the peak maximum shifts to a higher temperature with increasing frequency. In the frequency domain, the dipole loss peak of the mixture at 25 °C was located at 3 GHz. The dielectric constant in the frequency domain (in the range of dipole relax-

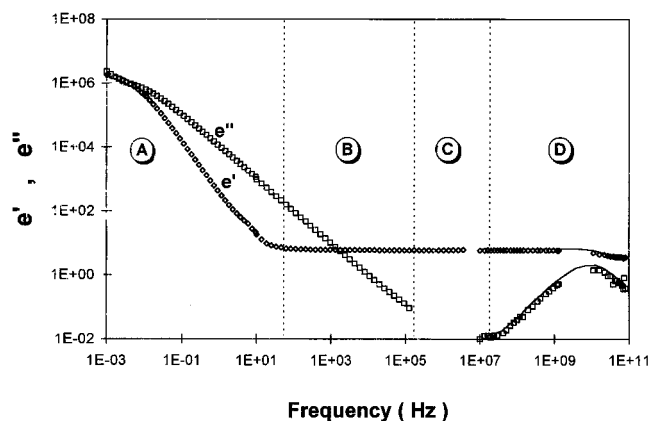


**Figure 2.** Dielectric constant and loss in the frequency domain for aniline at 25 °C. The symbols are actual data. Note the characteristic zones (A–D) of the dielectric response.

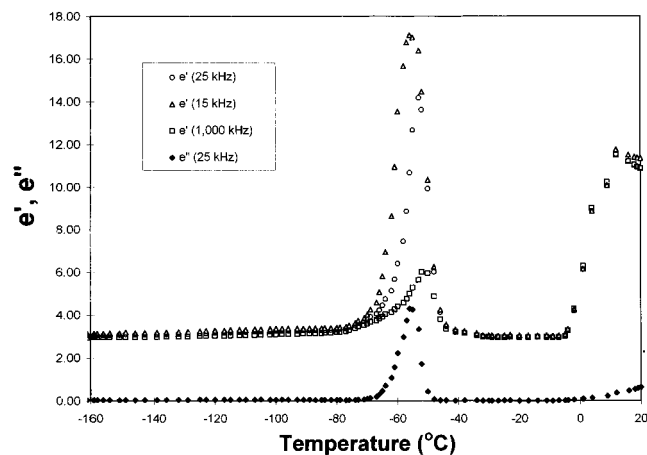


**Figure 3.** Dielectric constant and loss as a function of temperature with frequency as a parameter for PGE.

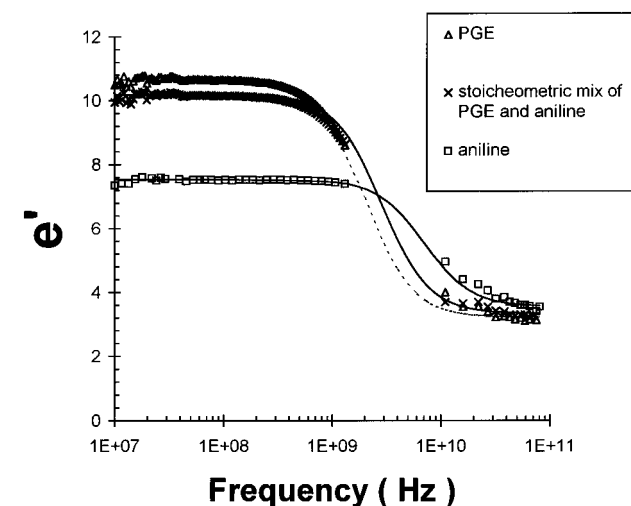


**Figure 4.** Dielectric constant in the frequency domain for PGE, aniline, and the PGE–aniline mixture at 25 °C.

ation) for PGE, aniline, and a non-reacted PGE–aniline mixture is plotted in Figure 4. The results of frequency sweeps on the nonreacted sample, performed at a series of temperatures, are shown in Figure 5. Interestingly and unexpectedly, the intensity of the loss peak was found to increase with increasing temperature, displaying a trend usually associated with  $\beta$  relaxation in polymers. This was attributed to the presence (detected by DSC) of some residual crystallinity in the nonreacted mixture. In partially reacted samples (at any conver-

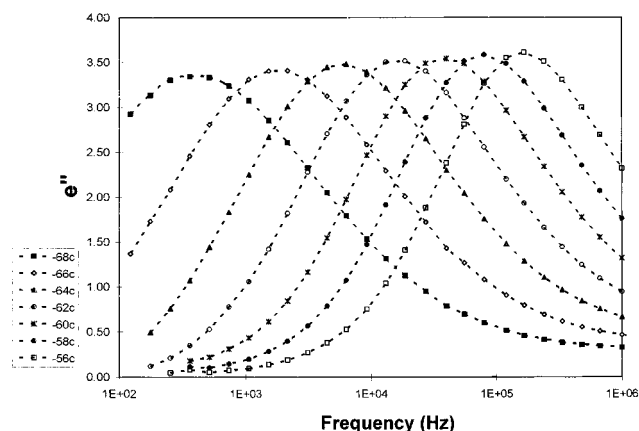


**Figure 5.** Dielectric loss in the frequency domain with temperature as a parameter for the PGE–aniline mixture prior to the onset of chemical reactions.

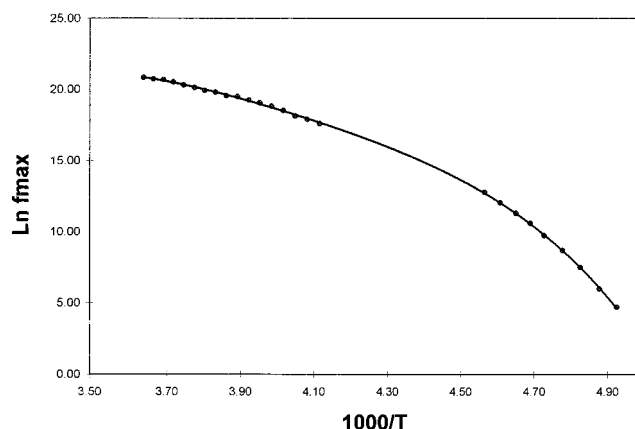


**Figure 6.** Frequency of dielectric loss peak maximum as a function of reciprocal temperature for the PGE–aniline mixture prior to the onset of chemical reactions.

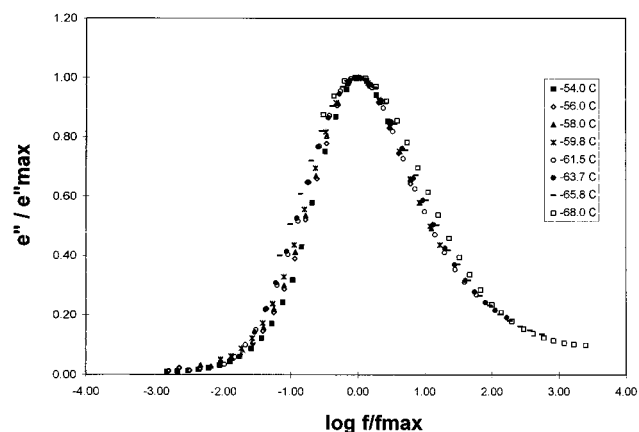


**Figure 7.** Normalized dielectric loss versus frequency at various temperatures for the PGE–aniline mixture prior to the onset of chemical reactions.

sion), however, this trend was absent, as all these samples were readily supercooled and showed no signs of residual or developing crystallinity during the frequency sweeps. A non-Arrhenius temperature dependence of the frequency of maximum loss was observed, as shown in Figure 6. Next, a normalized plot of dielectric loss versus frequency was constructed in an effort to extract the power law parameters  $m$  and  $n$  of Jonscher's model. The results, shown in Figure 7, suggest thermodielectric complexity (we use the term "thermodielectric complexity" in the same sense thermorheological complexity is invoked to describe the

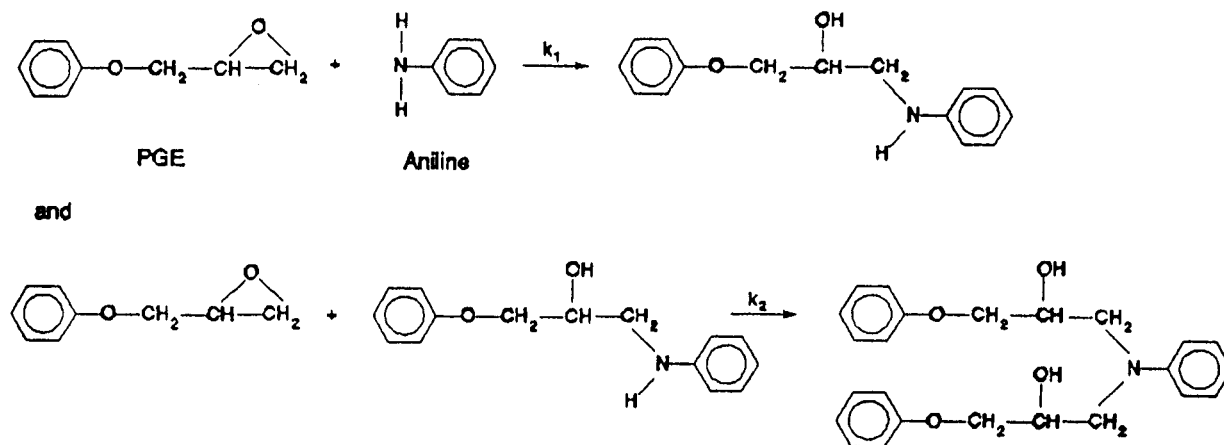


**Figure 8.** Chemical reaction in a PGE–aniline mixture.

dynamic mechanical response), thus precluding the use of Jonsher's approach in this case. This raises an intriguing question regarding the underlying cause for the observed thermoelectric complexity. An overlap between  $\alpha$  and  $\beta$  relaxations must be excluded as a possible explanation because these two relaxations do not overlap in the frequency–temperature window of Figure 7. We believe that the most likely source of thermoelectric complexity is the emergence of specific interactions that can alter the time scale of segmental motions. Hydrogen bonding, for instance, is an example of specific interactions that are present in the mixture and whose intensities are known to increase with decreasing temperature.

Let us now focus our attention on the systems that undergo chemical reactions. The reaction between PGE and aniline proceeds according to the two-step scheme shown in Figure 8, which is included as illustration only; the mechanism and kinetics of this reaction were established separately from the measurements by HPLC and remote fiber optic near infrared spectroscopy and were described in detail elsewhere.<sup>37,38</sup> For the purpose of the discussion that follows, it is sufficient to realize that an epoxy group reacts with a primary amine to form a secondary amine, which, in turn, reacts with another epoxy to give a tertiary amine. The effect of the progress of reaction on the reorientational dynamics was investigated by evaluating the dielectric response of a series of samples with precisely determined extents of reaction. For every run on a partially reacted mixture, we verified that no additional reactions took place in the course of a dielectric measurement. The results were highly reproducible and varied in a systematic manner as a function of temperature and frequency. A large number of runs were executed on samples with different extents of reaction, in Figure 9 we present data from the frequency sweeps between 0.1 kHz and 1 MHz for mixtures reacted to 20% (Figure 9a), 40% (Figure 9b), 60% (Figure 9c), and 100% (Figure 9d). The intensity of the loss peak is seen to decrease with an increase in the extent of reaction. It is also interesting to note that dielectric loss intensity was practically independent of temperature for any given extent of reaction with the exception of a fully reacted system (100% conversion, Figure 9d), where the loss peak intensity decreases with increasing temperature, in a trend common to most  $\alpha$  relaxation processes. For every extent of reaction other than 100%, however, a thermoelectrically complex response was obtained and hence we were again unable to evaluate the power law parameters of Jonsher's model. An example of high-

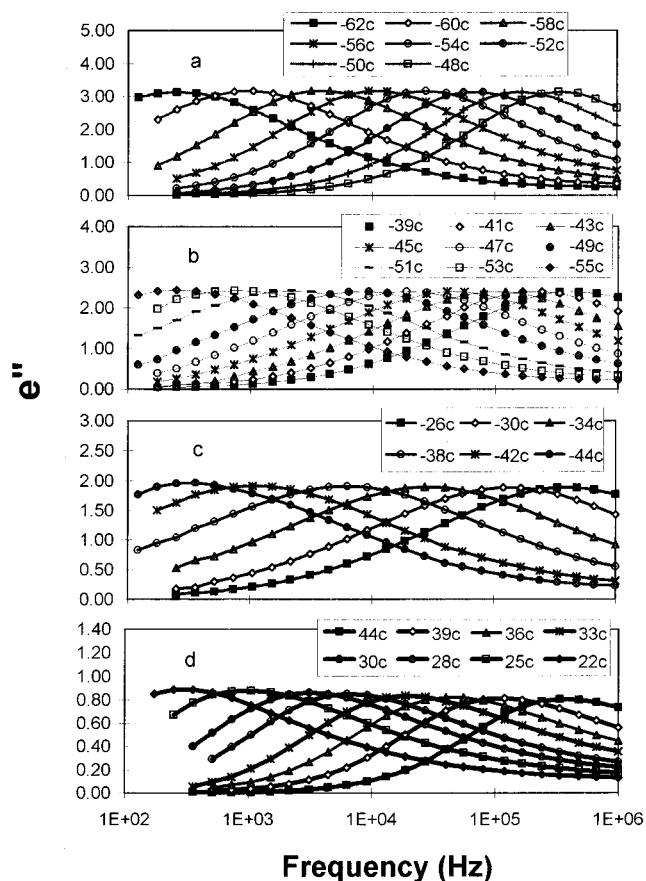


**Figure 9.** Dielectric loss in the frequency domain with temperature as a parameter for PGE–aniline mixtures reacted to (a) 20% conversion, (b) 40% conversion, (c) 60% conversion, and (d) 100% conversion.

frequency data is given in Figure 10. Here we show the dielectric constant (10A) and loss (10B) of a PGE–aniline mixture in the frequency domain with extent of reaction as a parameter. The mixture was reacted at 100 °C and then brought to 25 °C, where frequency sweeps were run. The  $\alpha$  relaxation peak shifts from its initial location at 3 GHz to lower frequency and becomes broader during reaction. We then proceeded to seek correlations between the observed changes in dielectric response and the molecular characteristics of the reactive mixture within the framework of the coupling theory. One way of utilizing the coupling theory to interpret one's findings and quantify the dispersion and temperature dependence of the segmental motions consists of constructing the fragility or cooperativity

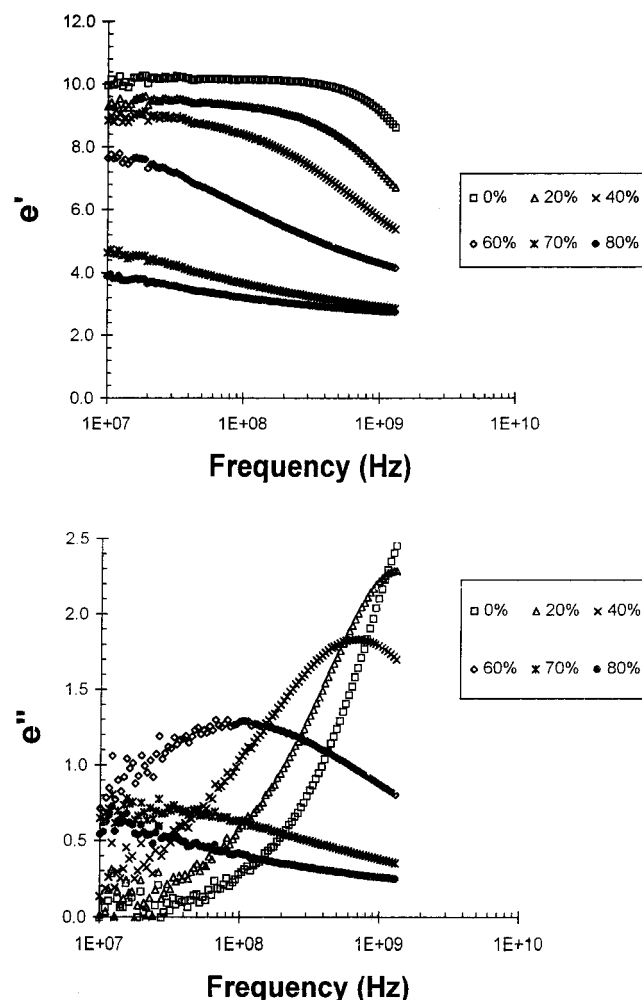


**Figure 10.** Dielectric constant and loss in the high-frequency domain with extent of reaction as a parameter. The mixture was reacted at 100 °C and swept at 25 °C.

plots, exploited first by Angell<sup>39</sup> and later by Ngai.<sup>40</sup> Cooperativity plots contain the most probable relaxation time as a function of normalized reciprocal temperature, expressed as  $T/T_g$  or  $(T - T_g)/T_g$ , where  $T_g$  is commonly taken to represent the temperature at which the relaxation time attains an arbitrary value between, e.g., 0.01 and 100 s. The shape and slope of these curves provide a measure of the extent of intermolecular cooperativity and have been shown by Roland and Ngai to vary as a function of chemical composition.<sup>41</sup> We reiterate, however, that the use of cooperativity plots to relate the progress of chemical reactions to the evolution of a new structure has not been reported hitherto. An examination of the cooperativity plot in Figure 11 affords a unique insight into the effect of the advancement of chemical reactions on dipole dynamics. We shall preface our interpretation of the cooperativity plot in Figure 11 by advancing an explanation of the nature of the various phenomena that govern cooperativity in reactive systems. We propose that the molecular-level characteristics that affect the intermolecular cooperativity of reactive systems can be classified into two categories: (1) **molecular architecture**, determined by symmetry, rigidity, and steric hindrance; and (2) **dielectric architecture**, determined by the type and concentration of dielectrically active species (mostly dipoles) and the various specific interactions that can affect the reorientational dynamics of dipoles. In general, an increase in the complexity of molecular architecture and in the

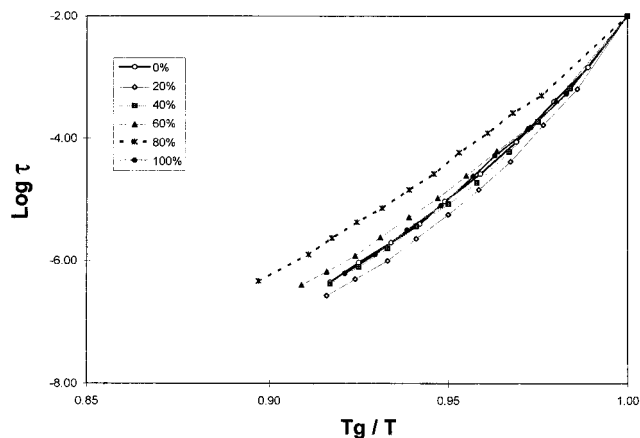


**Figure 11.** Cooperativity plot of relaxation time as a function of reduced temperature for PGE–aniline mixtures at various extents of reaction.

concentration of dielectrically active species should trigger an increase in cooperativity. The advancement of chemical reactions will certainly increase the rigidity and steric hindrance in the reactive mixture and should therefore cause an increase in the required cooperativity. For example, that explains why an increase in the concentration of cross-linker in poly(vinyl ethylene) results in a broader segmental relaxation dispersion and a steeper cooperativity plot, as described by Roland.<sup>42</sup> But while his study probed the effect of increasing concentration of a specific moiety on the cooperativity of an otherwise unchanged polymer, our systems are characterized by a change in both the concentration **and** the type of dielectrically active moieties as a result of chemical reactions. We recall that, in our model system, primary amine and epoxy groups react to form hydroxyl groups and secondary (early stage) and/or tertiary (later stage) amine groups, as shown in Figure 8. The key point to remember is that the character of these different dipoles and their contribution to intermolecular cooperativity are quite different. Reorientational motions of dipoles associated with epoxy and primary amine groups represent the molecular origin of  $\alpha$  relaxation and as such contribute directly to high intermolecular cooperativity. The reaction products in our model system, on the other hand, are very different; secondary and tertiary amines are less dielectrically active, while the hydroxyl group contributes to  $\beta$  relaxation and exerts a negligible influence on the  $\alpha$  relaxation in this system. This is readily seen in the multifunctional epoxy–amine formulations where the decrease in the intensity of  $\alpha$  relaxation is directly proportional to the concentration of epoxy groups.<sup>17</sup> In fact, the  $\alpha$  relaxation is completely suppressed in fully-cured systems, despite the abundance of hydroxyl groups. We also note that doping of DGEBA prepolymers (Table 2) with moisture had an effect on the  $\beta$  relaxation only. Thus, solely on the basis of the dielectric architecture of our mixture, i.e., the concentration and type of dipoles, one would expect a continuous decrease in cooperativity during reaction. This is contrary to the trend based solely on the molecular architecture, and hence we can say that, in our model system, molecular and dielectric architecture exert the opposite effect on the intermolecular cooperativity associated with  $\alpha$  relaxation during reaction. The overall direction in which the cooperativity shifts in the course of reaction is determined by the interplay of these two phenomena. Let us now examine how this information can be parlayed into the cooperativity plot of Figure 11.

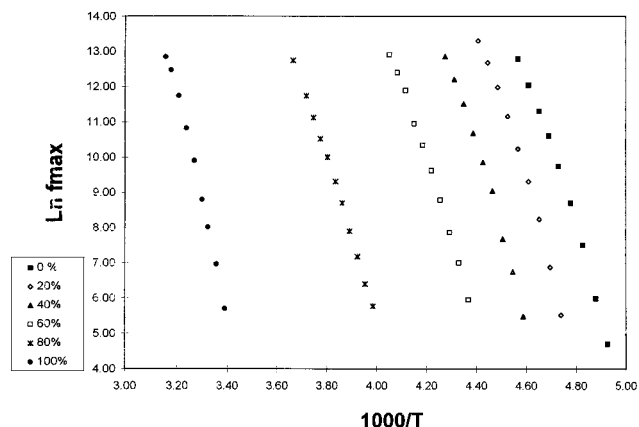


**Figure 12.** Natural log of the dielectric loss peak maximum as a function of reciprocal temperature for PGE–aniline mixtures reacted to 0, 20, 40, 60, 80 and 100% conversion.

The cooperativity of the nonreacted mixture reflects its initial molecular and dielectric architecture, the latter being strongly affected by mixing. Specific interactions are introduced upon mixing and these have an effect on the spatial distribution of dipoles associated with epoxy and primary amine groups and hence should influence the dielectric response. The presence of specific interactions due to mixing is further supported by infrared spectroscopy, which shows higher absorption by the epoxy (in particular) and primary amine groups in the nonreacted PGE–aniline mixture with an increase in temperature, contrary to the trend found in the individual components. Once the reactions begin, however, the effect of specific interactions diminishes rapidly. Between approximately 10 and 90% reaction there is a systematic decrease in cooperativity; the plot becomes less steep and its curvature decreases, as shown in Figure 11. We submit that in this range it is possible to explain the direction in which cooperativity shifts by considering the interplay between molecular and dielectric architecture. Specifically, we believe that the dominant influence on cooperativity between ca. 10 and 90% conversion is exerted by dielectric architecture, as the disappearance of major dipolar contributors to  $\alpha$  relaxation (epoxy and primary amine groups) outweighs the continuing demand for more cooperativity from the changing molecular architecture. Near and at the end of reaction (100%) the origin of dipole relaxations changes completely. The loss peak is still present, but its intensity is greatly reduced, as the origin of dipole relaxations now lies with less dielectrically active species, namely tertiary amines and glycidyl ethers. From the temperature dependence of the dielectric loss peak in the frequency domain at various extents of reaction, we constructed the corresponding activation energy plots shown Figure 12. All plots are non-Arrhenius in the frequency range between 100 Hz and 1 MHz.

**2. Effect of Molecular Weight of Epoxy Prepolymer on Reorientational Dynamics.** The second part of our model study examines the reorientational dynamics of a homologous series of bifunctional epoxies of different molecular weights described in Table 2. We note that an earlier study of the dielectric response in a series of epoxy prepolymers of different molecular weights has been reported by Sheppard and Senturia;<sup>43</sup> our principal goal was to complete the model compound study as a prelude to the investigation of network-forming epoxy–amine formulations<sup>17</sup> and to introduce the concept of cooperativity to data analysis. Various

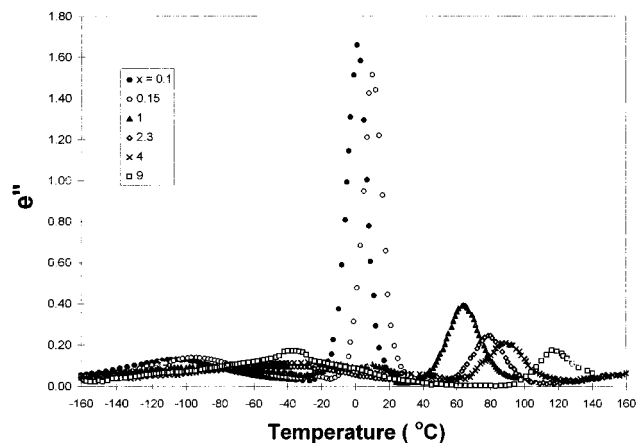


**Figure 13.** Dielectric loss as a function of temperature for six epoxy prepolymers of different molecular weights ( $x$  is the degree of polymerization).

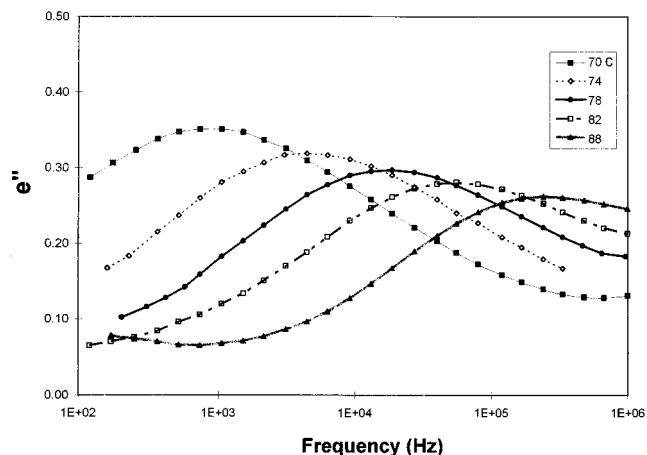


**Figure 14.** Dielectric loss in the frequency domain with temperature as a parameter for the epoxy prepolymer of degree of polymerization 2.3 (MW = 1380).

relaxation processes were observed in the frequency and temperature domains and are described below.

**a.  $\alpha$  Relaxation.** The molecular origin of  $\alpha$  relaxation in these epoxy prepolymers lies principally in the segmental motions associated with the dielectrically active terminal epoxy groups that are present in all DGEBA-type epoxies.

A composite plot of dielectric loss as a function of temperature for the six epoxy prepolymers investigated is shown in Figure 13. Data were generated at a constant frequency of 25 kHz and a prominent  $\alpha$  relaxation was present in each sample. The loss peak maximum shifts to a higher temperature, its breadth increases, and its intensity decreases with increasing molecular weight. A significant drop in the peak intensity was observed between the samples with degrees of polymerization of 0.15 and 1.

Frequency sweeps at various temperatures were performed on all prepolymers, and an example is given in Figure 14 for the prepolymer with the degree of polymerization of 2.3 (MW = 1380). The  $\alpha$  relaxation peak is clearly observed in the frequency domain; with increasing temperature, it shifts to higher frequency, while its intensity and dielectric dispersion decrease.

Next, the normalized plots of dielectric loss as a function of frequency were constructed for all prepolymers. The data superpose quite well, suggesting thermodielectric simplicity in the applied frequency interval between 0.1 kHz and 1 MHz, with the exception of the



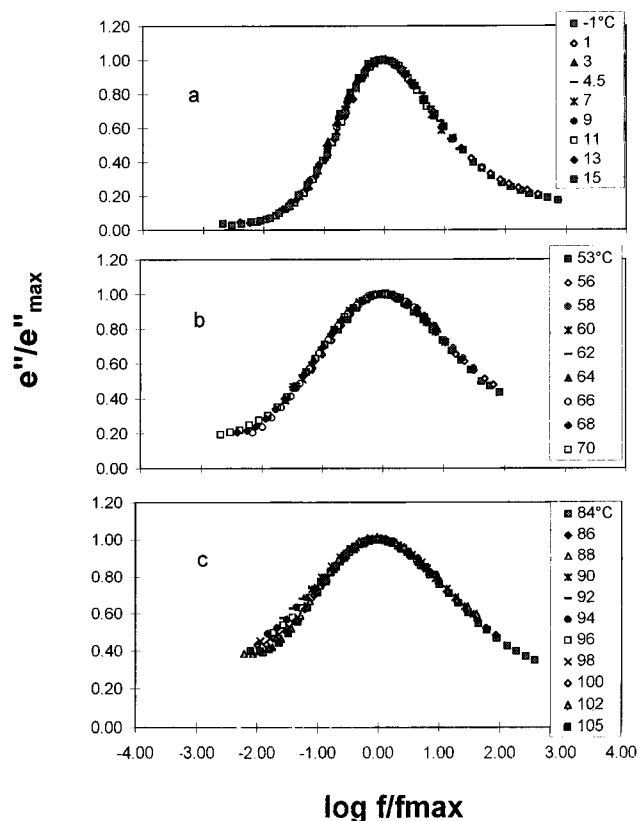


**Figure 15.** Normalized dielectric loss versus frequency at various temperatures for epoxy prepolymers with degrees of polymerization (a) 0.15, (b) 1, and (c) 4.

low-frequency tail of the prepolymer with the highest degree of polymerization ( $x = 9$ ; MW = 6100). Specific interactions are likely to cause this, and we are presently conducting an FTIR investigation of their nature. In Figure 15a–c we present these normalized plots for prepolymers with degrees of polymerization of 0.15, 1 and 4. The complete results for all prepolymers, expressed in terms of the power law parameters  $m$  and  $n$ , are summarized in Table 2. An increase in the prepolymer molecular weight results in a systematic decrease in the values of  $m$  and  $n$  and a concomitant increase in the breadth of the normalized distribution. In the spirit of Jonscher's theory, this trend is interpreted as a consequence of the increased rigidity in the samples of higher molecular weight. We also fit the data to the KWW equation, using the procedure described in the article that follows,<sup>17</sup> and examined how the empirical parameter  $\beta$  varied with molecular weight. A computer routine was used to solve for the best fit  $\beta$ , and our results were plotted as a function of molecular weight in Figure 16, together with the results reported by Sheppard and Senturia.<sup>43</sup> We observed a decrease in  $\beta$  with increasing molecular weight, and the two sets of data were in excellent agreement for molecular weights below 1380, as seen in Figure 16. For higher molecular weights, however, it was not possible to obtain satisfactory fits to the stretched exponential for our samples. Sheppard and Senturia, on the other hand, report a gradual increase in  $\beta$  to 0.39 (intuitively unexpected) with increasing molecular weight but show neither raw data nor fits, and hence, we have no way of estimating the accuracy of those values. It is also worth noting that drying under vacuum (Sheppard and Senturia did it and we did not) showed no effect on the  $\beta$  parameter.

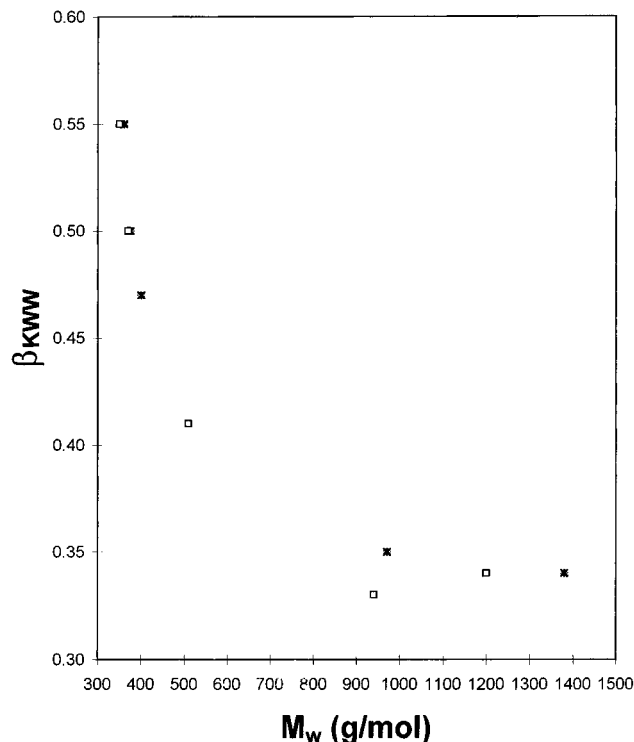


**Figure 16.** The KWW parameter  $\beta$  as a function of molecular weight: (\*) this study, (□) data from ref 43.

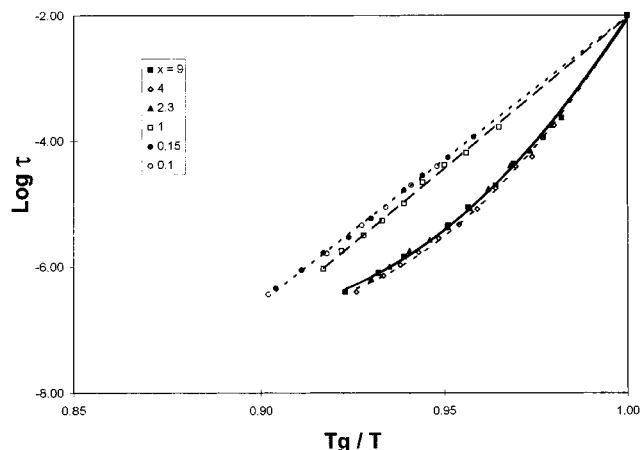


**Figure 17.** Cooperativity plot of relaxation time as a function of reduced temperature for six epoxy prepolymers of different molecular weights.

Finally, we sought to relate the observed changes in the dielectric response to the molecular and dielectric architecture of prepolymers within the framework of the coupling theory. The interpretation afforded by the cooperativity plot, shown in Figure 17 for all six prepolymers, is most interesting. In the frequency range from 100 Hz to 1 MHz we observe an Arrhenius type response for  $x \leq 1$  and a distinctly non-Arrhenius behavior for the higher molecular weight samples (naturally, all  $\alpha$  relaxations are inherently non-Arrhenius when viewed over 10 or more decades of frequency). We also report a curiously large increase in cooperativity in going from  $x = 1$  to  $x = 2.3$ ! Before attempting to interpret the observed results further, we had to consider the possible effect of two important parameters: the molecular weight distribution in a prepolymer and the presence of moisture. To answer the first question, all prepolymers were examined by size exclusion chromatography (SEC). For prepolymers with  $x = 0.1$ , 0.15, and 0.25 we observed a narrow molecular weight

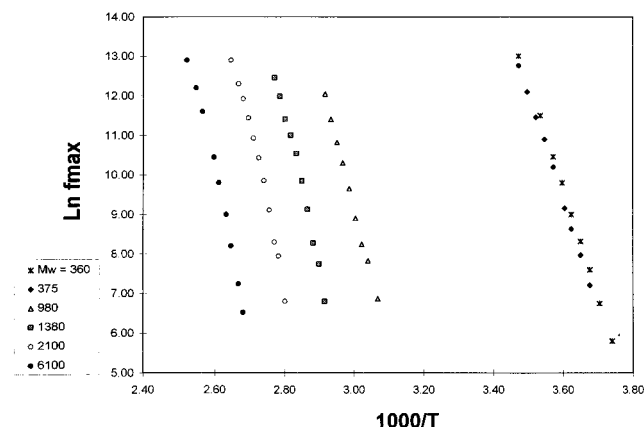


**Figure 18.** Frequency of dielectric loss peak maximum as a function of reciprocal temperature for six epoxy prepolymers with different degrees of polymerization.

distribution (MWD), whose breadth was indistinguishable from one sample to another. We therefore concluded that the observed effects on dynamics and cooperativity were not caused by MWD. Prepolymers of higher molecular weight ( $x > 0.25$ ) had a broader MWD but the breadth did not change with  $x$ , leading us again to conclude that the observed changes in dynamics are not due to the differences in the MWD. A small peak due to moisture was detected in the IR spectra of prepolymers with  $x \geq 2.3$ . Considering that the added moisture had no effect on the intensity of  $\alpha$  relaxation, that our samples were heated to above 100 °C prior to the frequency sweeps, and that our KWW  $\beta$  parameters agree very well with those of "dried" prepolymers,<sup>43</sup> we concluded that the presence of moisture at the conditions of this study did not play a significant role in the dynamics of the  $\alpha$  process. It is also interesting to note that the effects of molecular and dielectric architecture on cooperativity are similar for the group of prepolymers with  $x \leq 1$  and the group with  $x \geq 2.3$ . It is possible that the change in molecular weight between  $x = 1$  and  $x = 2.3$  (no difference in the MWD) brings about the observed increase in cooperativity owing to the dominant influence of the dielectric architecture (increase in the intensity of specific interactions due to hydrogen bonding) over the molecular architecture. Our current efforts are focused on quantifying these concepts. Finally, it is worth noting that the large gap between the samples with  $x = 0.15$  and  $x = 1$ , observed in the activation energy plot of Figure 18, is primarily the result of higher  $T_g$ ; this suggests that  $T_g$  alone is not sufficient in describing cooperativity in reactive systems. In sum, both the power law concept and the coupling theory can be used to rationalize the experimentally observed trends in a homologous series of bifunctional epoxy prepolymers of different molecular weights.

**b. Secondary Relaxations.** The secondary relaxations ( $\beta$ ,  $\gamma$ , etc.) in polymers and oligomers result from the localized motions in the main chain and/or side groups in the glassy state. Most published studies on epoxy resins report a single  $\beta$  relaxation, whose molecular origin is seldom examined and yet invariably assigned to the local motions within the  $-\text{O}-\text{CH}_2-\text{CHOH}-\text{CH}_2-$  moiety.<sup>44–46</sup> In this study, however, we have identified three peaks below the  $\alpha$  peak and have utilized a number of model compounds in order to elucidate the molecular origin of these relaxation processes. An example of our results is the plot of dielectric loss versus temperature at 25 kHz for the epoxy

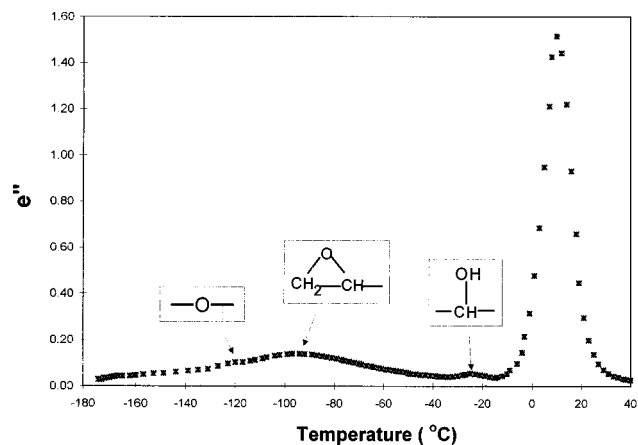


**Figure 19.** Dielectric loss as a function of temperature for the prepolymer with  $x = 0.15$ . Note the presence of three secondary relaxation peaks.

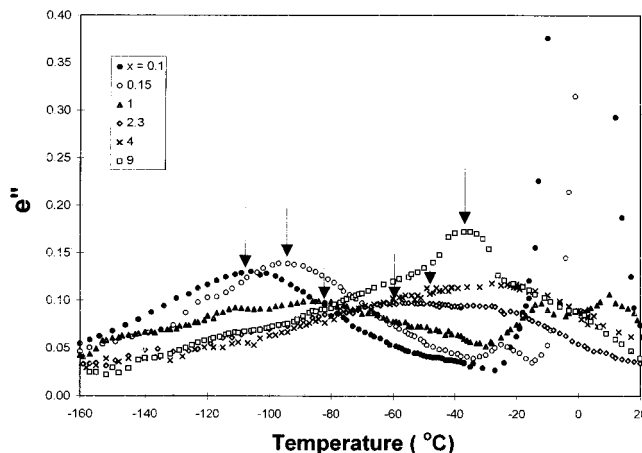


**Figure 20.** Dielectric loss as a function of temperature with prepolymer molecular weight as a parameter.

prepolymer with degree of polymerization  $x = 0.15$ , shown in Figure 19.

The lowest temperature peak is centered around  $-120$  °C. This relaxation, termed  $\delta$ , was consistently observed in all ether-containing compounds and is thence associated with the motions of the ether unit. The intensity of this peak was invariably weak and its location did not vary with molecular weight. The highest temperature peak, located at around  $-30$  °C, is related to the relaxation of hydroxyl units and was labeled  $\beta$ . The intensity of this peak increases considerably with an increase in molecular weight, as clearly seen in the composite plot of Figure 20. The peak maximum falls within a narrow temperature range but does not vary in a systematic fashion as a function of molecular weight. This peak has been associated in the literature with the local motions within the  $-\text{O}-\text{CH}_2-\text{CHOH}-\text{CH}_2-$  moiety, although that assignment is questionable. For instance, the addition of a small amount of water has little effect on the temperature at loss peak maximum, while causing a measurable increase in the peak intensity. The sensitivity of this peak to the presence of hydroxyl groups suggests that these groups may be at the origin of the  $\beta$  relaxation.

The most prominent secondary relaxation in epoxy prepolymers with  $x \leq 1$  was observed at  $-95$  °C (see Figure 19). We term this process  $\gamma$  relaxation. The molecular origin of this relaxation lies in the localized motions within the epoxy ring. Naturally, this should not be confused with the segmental motion of terminal

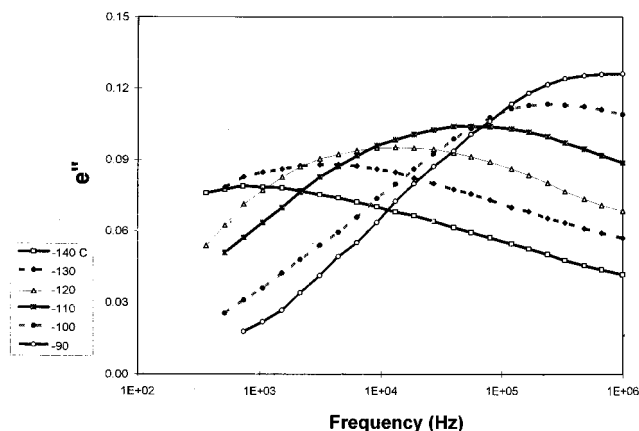


**Figure 21.** Dielectric loss ( $\gamma$  relaxation) in the frequency domain with temperature as a parameter for the prepolymer with  $x = 0.1$ .

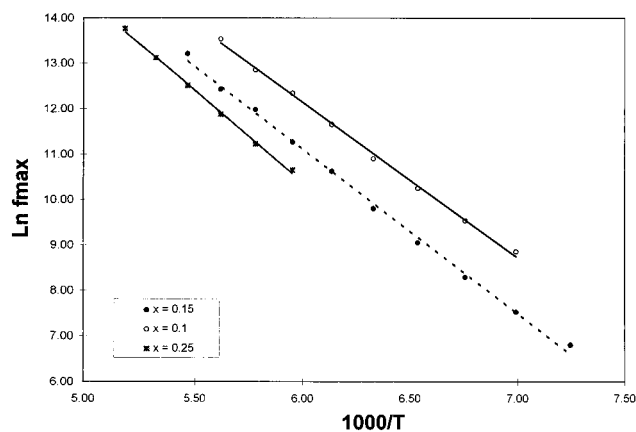


**Figure 22.** Frequency of dielectric  $\gamma$  loss maximum as a function of reciprocal temperature for prepolymers with  $x = 0.1, 0.15$ , and  $0.25$ .

epoxy groups on glycidyl moieties that causes  $\alpha$  relaxation. The  $\gamma$  relaxation peak shifts to a higher temperature and decreases in intensity with increasing molecular weight, a result of the lower concentration of terminal epoxy groups per unit volume. The upward shift of the  $\gamma$  peak, observed in the higher molecular weight samples ( $x \geq 1$ ) and marked by arrows in Figure 20, is caused by the overlap between  $\beta$  and  $\gamma$  processes.

Frequency sweeps were performed next in order to isolate and quantify the observed  $\gamma$  process. An example of the dielectric  $\gamma$  relaxation in the frequency domain for the prepolymer with  $x = 0.1$  is shown in Figure 21. The loss peak maximum shifts to higher frequency and its intensity increases with increasing temperature. We calculated the activation energy of prepolymers with  $x = 0.1, 0.15$ , and  $0.25$  and found them to be 6.75, 7.50, and 8.00 kcal/mol, respectively. All three prepolymers displayed an Arrhenius response, as shown in Figure 22. The calculated activation energies fall within the range of reported values for  $\gamma$  and  $\beta$  processes, between 4 and 23 kcal/mol.<sup>47</sup> Reliable values of activation energy for the higher molecular weight prepolymers were difficult to obtain because of much weaker loss intensity and the overlap between  $\gamma$  and  $\beta$  processes.

A normalized plot of dielectric loss versus frequency for the prepolymer with  $x = 0.15$  was constructed and depicted in Figure 23. This and the other two prepolymers ( $x = 0.1$  and  $0.25$ ) were found to be thermodielectrically simple and the slopes of their low- and high-frequency linear portions of the normalized loss were

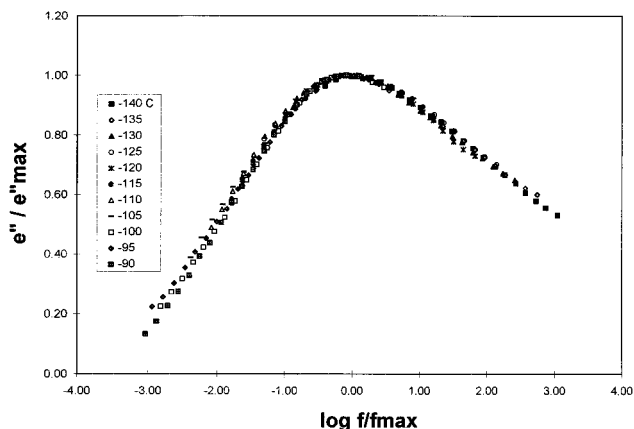


**Figure 23.** Normalized dielectric loss versus frequency at various temperatures for the epoxy prepolymer with degree of polymerization  $x = 0.15$ .

lower in the higher molecular weight prepolymer. These findings were interesting and have raised important questions regarding the fundamental nature of  $\beta$  and  $\gamma$  relaxations. Are these processes truly noncooperative, as usually assumed, or is it possible that some localized cooperativity requirements are introduced as a result of, e.g., the hydrogen bonding that involves terminal epoxy groups? Is there a fundamental correlation between the breadth of the distribution (as measured by the KWW parameter  $\beta$  or Jonscher's parameters  $m$  and  $n$ ) of  $\beta$  and  $\gamma$  relaxation processes and the molecular and dielectric architecture of the molecule? Such an investigation is currently underway in our laboratory.

## Conclusions

We have investigated the effects of progress of the reaction and prepolymer molecular weight on the reorientational dynamics of model epoxy–amine systems. Experimental results were generated over a wide range of frequency and temperature, and an explanation for the observed findings was put forward within the framework of the coupling theory and intermolecular cooperativity.

The manner in which the intermolecular cooperativity varies in the course of reaction is determined by the interplay between two inherent molecular characteristics of a reactive system, its molecular and dielectric architecture. The former is determined by the symmetry, intra- and intermolecular rigidity, and steric hindrance, while the latter depends on the type and concentration of dielectrically active species.

An increase in the prepolymer molecular weight increases cooperativity, but not linearly. The abrupt increase in cooperativity observed between prepolymers with degrees of polymerization of 1 and 2.3 was caused by an increase in the concentration of the dielectrically active hydroxyl groups and a concomitant increase in intermolecular rigidity. An increase in the glass transition temperature does not translate directly into higher cooperativity.

The variation in cooperativity during reaction is more complex. The initial cooperativity of the nonreacted mixture is high owing to the specific interactions introduced upon mixing and confirmed by infrared spectroscopy. These interactions, however, weaken during the early stages of the reaction; from that point on, the cooperativity plot reflects correctly the interplay between molecular and dielectric architecture and can

be used to explain the dynamics of reactive systems. This holds true for the conversion range between approximately 10 and 85%. The major driving force for cooperativity in that conversion range is the segmental motions of terminal epoxy groups on glycidyl moieties. A fully reacted system represents a different material with its own cooperativity requirements and should be viewed as such.

**Acknowledgment.** This material is based on work supported by the National Science Foundation under Grant No. DMR-9400716.

## References and Notes

- (1) Williams, G. *Adv. Polym. Sci.* **1979**, *39*, 59.
- (2) McKenna, G. B. *Glass Formation and Glassy Behavior. Comprehensive Polymer Science, Vol. 2, Polymer Properties*; Pergamon: Oxford, U.K., 1989.
- (3) Adachi, K.; Yoshida, H.; Fujui, F.; Kotaka, Y. *Macromolecules* **1990**, *23*, 3138.
- (4) Boese, D.; Kremer, F. *Macromolecules* **1990**, *23*, 829.
- (5) Ngai, K. L.; Roland, M. *Macromolecules* **1992**, *24*, 5315.
- (6) Ngai, K. L.; Roland, M. *Macromolecules* **1993**, *26*, 6824.
- (7) Watanabe, H.; Yamada, H.; Urakawa, O. *Macromolecules* **1995**, *28*, 6443.
- (8) Inoue, T.; Cicerone, M. T.; Ediger, M. D. *Macromolecules* **1995**, *28*, 3425.
- (9) Hofmann, A.; Alegria, A.; Colmenero, J.; Willner, L.; Buscaglia, E.; Hadjichristidis, N. *Macromolecules* **1996**, *29*, 129.
- (10) Garwe, F.; Schonhals, A.; Lockwenz, H.; Beiner, M.; Schroter, K.; Donth, E. *Macromolecules* **1996**, *29*, 247.
- (11) The most recent coverage of current issues has been presented at the Symposium on Glasses and Glass Formers, held during the Fall 1996 meeting of the Materials Research Society, Boston, MA, December 2–6, 1996: *MRS Symposium Proceedings*; Elsevier: New York, 1997; Vol. 455.
- (12) Kranbuehl, D. E.; Delos, S. E.; Jue, P. K. *Polymer* **1986**, *27*, 11.
- (13) Senturia, S. D.; Sheppard, N. F. *Adv. Polym. Sci.* **1986**, *80*, 1.
- (14) Nass, K. A.; Seferis, J. C. *Polym. Eng. Sci.* **1988**, *29*(5), 315.
- (15) Mangion, M. B. M.; Johari, G. P. *J. Polym. Sci., Part B: Polym. Phys. Ed.* **1991**, *29*, 1117.
- (16) Fournier, J.; Williams, G.; Duch, C.; Aldridge, G. A. *Macromolecules* **1996**, *29*, 7097.
- (17) Andjelic, S.; Fitz, B.; Mijovic, J. *Macromolecules* **1997**, *30*, 5239 (following paper in this issue (and references therein)).
- (18) Stockmayer, W. H. *Pure Appl. Chem.* **1967**, *15*, 539.
- (19) Imanishi, Y.; Adachi, K.; Kotaka, T. *J. Chem. Phys.* **1988**, *89*, 7585.
- (20) Boese, D.; Kremer, F.; Fetters, L. J. *Macromolecules* **1990**, *23*, 1826.
- (21) Watanabe, H.; Urakawa, O.; Kotaka, T. *Macromolecules* **1993**, *26*, 5073.
- (22) Matsuoka, S.; Roe, R. J.; Cole, H. F. in *Dielectric Properties of Polymers*; Karasz, F. E., Ed.; Plenum Press: New York, 1972; p 255.
- (23) Mijovic, J.; Andjelic, S.; Yee, W. C. F.; Bellucci, F.; Nicolais, L. *Macromolecules* **1995**, *28*, 2797.
- (24) Mijovic, J.; Bellucci, F.; Nicolais, L. *J. Electrochem. Soc.* **1995**, *142*, 1176.
- (25) Mijovic, J.; Yee, W. C. F.; Carin, L. *Polym. News* **1993**, *18*, 364.
- (26) Fitz, B. MS Thesis in Polymer Science and Engineering, Polytechnic University, 1995.
- (27) Mijovic, J.; Andjelic, S. *Macromolecules* **1995**, *28*, 2789.
- (28) Floudas, G.; Placke, P.; Stepanek, P.; Brown, W.; Fytas, G.; Ngai, K. L. *Macromolecules* **1995**, *28*, 6799.
- (29) Adam, G.; Gibbs, J. H. *J. Chem. Phys.* **1965**, *43*, 139.
- (30) For a recent review see: Ngai, K. L. In *Disorder Effects on Relaxation Processes*; Richert, R.; Blumen, A., Eds.; Springer-Verlag: Berlin, 1994; pp 89–150.
- (31) Jonscher, A. K. *Dielectric Relaxation in Solids*; Chelsea Dielectric Press: London, 1983.
- (32) Gotze, W. *Z. Phys.* **1985**, *B60*, 195.
- (33) S. Matsuoka, S. *Relaxation Phenomena in Polymers*; Hanser Publishers: Munich 1992.
- (34) Zorn, R.; Arbe, A.; Colmenero, J.; Frick, B.; Richter, D.; Buchenau, U. *Phys. Rev. E* **1995**, *52*, 781.
- (35) Dissado, L. A.; Hill, R. M. *Nature* **1979**, *279*, 685.
- (36) Roland, M. *Macromolecules* **1995**, *28*, 3463.
- (37) Mijovic, J.; Fishbain, A.; Wijaya, J. *Macromolecules* **1992**, *25*, 979.
- (38) Mijovic, J.; Andjelic, S.; Kenny, J. M. *Polym. Adv. Technol.* **1996**, *7*, 1.
- (39) Angell, C. A. *J. Non-Cryst. Solids* **1991**, *131–133*, 13.
- (40) Plazek, D. J.; Ngai, K. L. *Macromolecules* **1991**, *24*, 1222.
- (41) For a recent review see: Ngai, K. L.; Plazek, D. J. *Rubber Chem. Technol.* **1996**, *68*, 376.
- (42) Roland, C. M. *Macromolecules* **1994**, *27*, 4242.
- (43) Sheppard, N. F.; Senturia, S. D. *J. Polym. Sci., Part B: Polym. Phys.* **1989**, *27*, 753.
- (44) Pochan, J. M.; Gruber, R. J.; Pochan, D. F. *J. Polym. Sci., Polym. Phys. Ed.* **1981**, *19*, 149.
- (45) Mijovic, J.; Tsay, L. *Polymer* **1982**, *22*, 902.
- (46) Butta, E.; Livi, A.; Levita, G.; Rolla, P. *J. Polym. Sci., Part B: Polym. Phys.* **1995**, *33*, 2253.
- (47) Hedvig, P. *Dielectric Spectroscopy of Polymers*; Wiley: New York, 1977.

MA970009U